Inorganic Chemistry
Article
pubs.acs.org/IC

Anion-Dependent Assembly of Four Sensitized Near-Infrared Luminescent Heteronuclear Zn^{II}−Yb^{III} Schiff Base Complexes from a Trinuclear Zn^{II} Complex

Zhi-Peng Zheng,[†] Yan-Jun Ou,[†] Xu-Jia Hong,[†,‡] Lei-Ming Wei,[†] Lin-Tao Wan,[†] Wo-Hua Zhou,[†] Qing-Guang Zhan,[†] and Yue-Peng Cai*,[‡]

[†]Guangzhou Key Laboratory of Materials for Energy Conversion and Storage, School of Chemistry and Environment, South China Normal University, Guangzhou 510006, P.R. China

[‡]State Key Laboratory of Structure ChemistryFujian Institute of Research on the Structure of Matter, Chinese Academy of Sciences, Fuzhou 350002, P.R. China

Supporting Information

ABSTRACT: Four anion-dependent 0D Zn^{II}−Yb^{III} heterometallic Schiff base complexes, $[YbZn_2L_2(OAc)_4]\cdot ClO_4$ (**2**), $YbZnL_2(NO_3)_3$ (**3**), $[(YbL)_2(H_2O)Cl(OAc)]_2\cdot[ZnCl_4]_2$ (**4**), and $YbZnL(OAc)_4$ (**5**), were assembled through central metal substitution or reconstruction from homotrinuclear Zn^{II} complex $\{[(Zn(OAc)(H_2O)L]_2Zn\}(ClO_4)_2\cdot 4H_2O$ [**1**; HL = 2-ethoxy-6-[(pyridin-2-ylmethylimino)methyl]phenol] with different $Yb^{III}X_3$ salts [X = ClO_4 (**2**), NO_3 (**3**), Cl (**4**), and OAc (**5**)], in which the Zn^{II}-sensitized near-infrared luminescent performances in the four complexes **2**−**5** are closely related to their structural models.

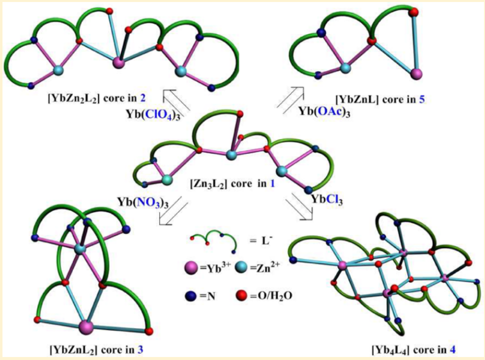

1. INTRODUCTION

Considering a low absorption coefficient and narrow line-like emission bands from f−f transition of lanthanide coordination systems, the luminescence of Ln^{III} ions is mostly achieved through an indirect sensitization process from light-harvesting antenna chromophores instead of direct excitation of the Ln^{III} centers.[1] As a result, in addition to the rational design of organic aromatic ligands directly bound to the lanthanide centers,[2] it is well-known that introducing other metal ions such as Cr^{II},[3] Ru^{II},[4] Ir^{III},[5] Pd^{II}/Pt^{II},[6] Zn^{II},[7] and Cd^{II} [8] as sensitizers into lanthanide complexes is also another commonly utilized strategy to sensitize lanthanide luminescence.[1] Among the reported metals as sensitizers, platinum, ruthenium, palladium, and iridium are expensive and cadmium and chromium are environmentally unfriendly, because of which Zn^{II} is more frequently chosen as a sensitizer for Ln^{III}-based NIR emission; therefore, the design and construction of Zn 4f heterometallic complexes have been receiving extensive attention in recent years.[1,7,9]

In order to effectively construct near-infrared (NIR) luminescent heteronuclear Zn 4f complexes, meanwhile, considering different affinities of zinc and 4f atoms for oxygen and nitrogen donors, a new Schiff base ligand of 2-ethoxy-6-[(pyridin-2-ylmethylimino)methyl]phenol (HL; Scheme 1) with pyridine and *o*-ethylvanillin substituents is deliberately designed and synthesized from the condensation of pyridin-2-ylmethanamine with 3-ethoxy-2-hydroxybenzaldehyde.[10] Compared to the well-studied salen-type Schiff base ligands in 3d−4f heteronuclear complexes,[11] the new ligand HL exhibits a distinct advantage, namely, the five/six-membered chelating rings fused together with pyridine and benzene rings via the common side of the polygons after coordination to transition metals to easily form one delocalized *π*-conjugated system as the chromophore (Scheme S1 in the Supporting Information, SI) and facilitate energy transfer between 3d and 4f metals, further sensitizing luminescence of lanthanide complexes.

Scheme 1. Molecular Structure of the Schiff Base Ligand HL

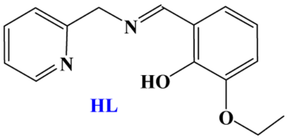

On the basis of this background, we herein designed and successfully assembled four anion-dependent heteronuclear Zn^{II}−Yb^{III} complexes, $[YbZn_2L_2(OAc)_4]\cdot ClO_4$ (**2**), $YbZnL_2(NO_3)_3$ (**3**), $[(YbL)_2(H_2O)Cl(OAc)]_2[ZnCl_4]_2$ (**4**), and $YbZnL(OAc)_4$ (**5**), through central metal substitution or reconstruction from homotrinuclear Zn^{II} complex $\{[(Zn(OAc)(H_2O)L]_2Zn\}(ClO_4)_2\cdot 4H_2O$ (**1**) as the starting material and different $Yb^{III}X_3$ salts [X = ClO_4 (**2**), NO_3 (**3**), Cl (**4**) and

Received: May 13, 2014
Published: August 26, 2014

OAc (**5**); Scheme 2]. Further investigative results show that the introduction of a Zn^{II} ion can effectively sensitize NIR luminescent performances in complexes **2**−**5**, which are closely related to the reaction counterions. Moreover, using a stepwise reaction is aimed at avoiding the disadvantage of Schiff base ligands in the process of assembling metal complexes such as hydrolysis and destruction due to excess metal cations.[10,12] Also, after 3 days, pale-yellow block crystals (**1**−**5**) were obtained by slow cooling to room temperature, and their compositions were determined through elemental analysis and single crystal/powder X-ray structure determination (see the SI).

Scheme 2. Assembling Strategies of Complexes 2−5

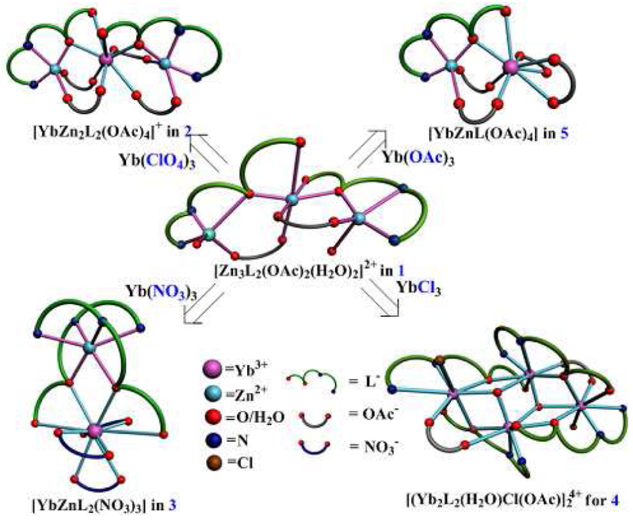

2. RESULTS AND DISCUSSION

Crystal Structures. The reaction of $Zn(OAc)_2 \cdot 2H_2O$ and $NaClO_4$ with HL in a 1:1:1 ratio in methanol afforded pale-yellow crystals. Single-crystal analysis revealed that compound **1** crystallized in triclinic space group $P\overline{1}$. A perspective view of the cationic structure of compound **1** is presented in Figure 1. There are three Zn^{II} ions in the asymmetric unit of **1**, in which Zn1/Zn3 atoms were pentacoordinated to two nitrogen atoms (N1/N3 and N2/N4), one hydroxyl oxygen atom (O1/O3) from one deprotonated ligand L$^-$, one acetic oxygen atom (O5/O9), and one coordinated water molecule (O7/O10), showing a distorted square-pyramidal coordination geometry. Zn2 was placed between Zn1 and Zn3 and sexacoordinated with the two phenol oxygen atoms (O1/O3), two ethoxyl oxygen atoms (O2/O4) from two adjacent ligands, and two μ_2-bridging acetic groups (O6/O8), presenting a distorted octahedral coordination geometry. The cationic trinuclear Zn3 unit with two positive charges was further connected to two perchlorate anions and four water molecules via intermolecular C(O)−H···Cl hydrogen bonds to form a 3D supramolecular chain (Figure S1 and Table S1 in the SI).

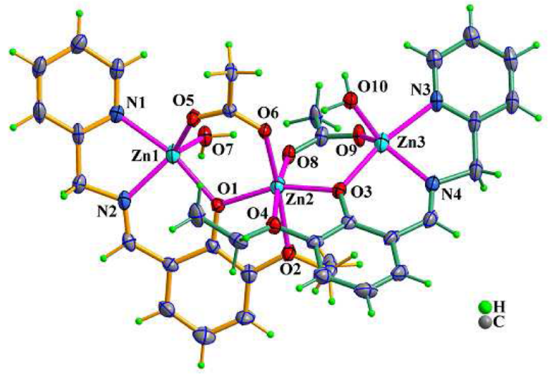

Figure 1. Perspective view of the cationic $\{[(Zn(OAc)L(H_2O)]_2Zn\}^{2+}$ in **1** with a partial atomic numbering scheme and their displacement ellipsoids at 20% probability.

When compound **1** as the starting material reacted with $Yb(ClO_4)_3$ under the same reaction conditions, one new pale-yellow prism complex, **2**, was obtained, and its cationic structure is depicted in Figure 2. The structure shows that **2** crystallized in orthorhombic space group *Pbca*. It could be simply viewed as one substitution of the central Zn^{II} ion with the Yb^{III} ion via two more μ_2-bridging coordinated acetates instead of two coordinated water molecules in **1**, possibly derived from the fact that lanthanide Yb^{III} prefers to coordinate to oxygen in the present case. Therefore, the distorted bicapped trigonal-prismatic coordination geometry of the central Yb1 atom was satisfied by four oxygen atoms from four μ_2-bridging acetate anions (O6, O8, O9, and O11) and the remaining four oxygen atoms (O1, O2, O3, and O4) from two hydroxyl (O1 and O3) and two ethoxyl oxygen atoms (O2 and O4) of two deprotonated ligands L$^-$ with an average Yb−O distance of 2.325 Å. Similar to **1**, both Zn1 and Zn2 atoms in **2** are pentacoordinated and present a distorted square-pyramidal coordination geometry.

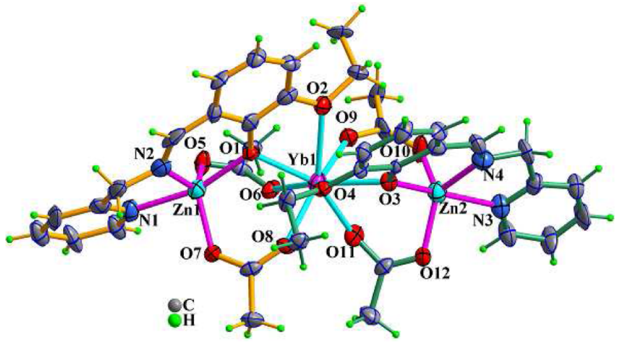

Figure 2. Perspective view of the cationic $\{[(Zn(OAc)_2L]_2Yb\}^+$ in **2** and their displacement ellipsoids at 20% probability.

Utilizing $Yb(NO_3)_3$ as the starting material instead of $Yb(ClO_4)_3$, compound **3** was generated via the destruction and reconstruction of compound **1**. Compound **3** crystallized in monoclinic space group *C*2/*c*, and one molecular unit contains one Zn^{II} ion, one Yb^{III} ion, three chelating nitrate ions, and two deprotonated ligands L$^-$, which approached each other to create an inner N2O4 crown and an outer O4-crown cave. With different preference for nitrogen and oxygen atoms, Zn1 occupied the inner N2O4-crown cave, presenting a distorted octahedral coordination geometry, while the Yb1 atom was trapped in the outer O4-crown cave with three chelating coordinated nitrate ions as the terminal ligands to meet its decacoordinated need, forming heterobinuclear complex **3**, as indicated in Figure 3.

When $YbCl_3$ is taken as the starting material instead of $Yb(ClO_4)_3$, the same reaction can also cause destruction of

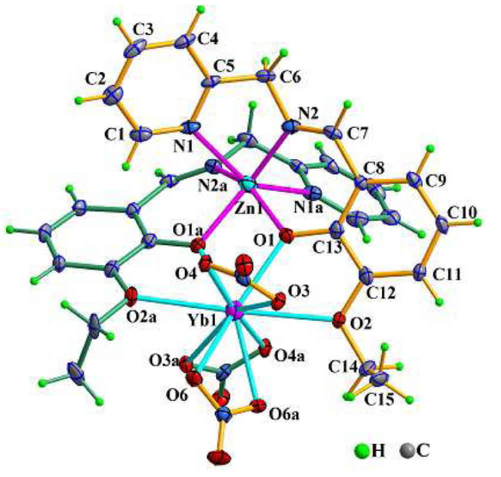

Figure 3. Perspective view of **3** with partial atomic labels and their displacement ellipsoids at 20% probability.

compound **1** under the same reaction conditions to give new compound **4**. Single-crystal X-ray diffraction shows that **4** is an ionic-type complex, composed of one cationic $[(YbL)_2(H_2O)Cl(OAc)]_2^{4+}$ unit and two anionic $[ZnCl_4]^{2-}$ moieties correlated with each other by C−H···Cl hydrogen bonds (Figure S2 and Table S1 in the SI). The cationic part is a centrosymmetric tetraytterbium moiety consisting of two asymmetric binuclear $[Yb_2L(H_2O)Cl(OAc)]^{3+}$ units linked by two μ_3-bridging water molecules, two μ_2-OAc$^-$ anions, and two deprotonated ligands L$^-$, as depicted in Figure 4, in which its

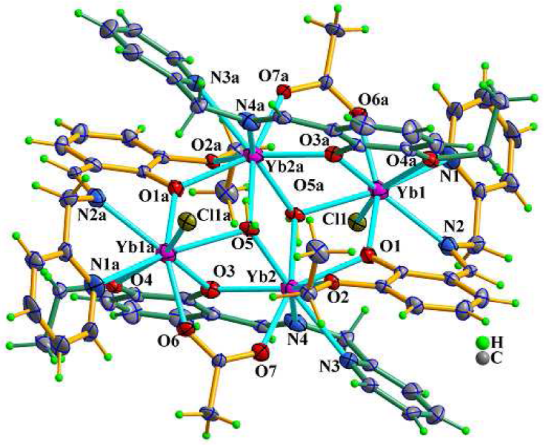

Figure 4. Perspective view of the cationic $[(YbL)_2(H_2O)Cl(OAc)]_2^{4+}$ in **4** with partial atomic labels and their displacement ellipsoids at 20% probability. Symmetric code: (a) $1 - x$, $2 - y$, $1 - z$.

central core Yb_4O_6 presents two reversely oriented face-sharing defect cubanes formed via the coordination of four μ_2-O and two μ_3-O atoms to four coplanar Yb^{III} atoms (Figure S3 in the SI). The two atoms Yb1/Yb2 are octacoordinated by two imine nitrogen atoms (N1, N2/N3, and N4), three oxygen atoms (O1, O3a, O4a/O1, O2, and O3) from two adjacent deprotonated ligands L$^-$, two oxygen atoms each from μ_2-bridging acetate and μ_3-bridging water molecule, the remaining chloride for Yb1 and the one symmetry-related μ_3-bridging water molecule (O5a) for Yb2, showing the same slightly distorted bicapped trigonal-prismatic coordination geometries with the normal ranges of Yb−O and Yb−N bond lengths. However, the anionic $[ZnCl_4]^{2-}$ unit is merely tetracoordinated to four terminal chlorides, presenting a simple tetrahedral coordination geometry (Figure S4 in the SI). Two parts of the cationic and anionic moieties are correlated with each other by C−H···Cl hydrogen bonds and further expanded into a 2D supramolecular layer in the *ac* plane (Figure S5 and Table S1 in the SI).

Because $Yb(OAc)_3$ was used as the beginning reactant, binuclear compound **5** was obtained. Single-crystal analyses reveal that compound **5** crystallized in triclinic space group $P\overline{1}$ and could be viewed as a replacement for one zinc/ligand unit of compound **2** with two terminal acetic groups. Its asymmetric unit contains two crystallographically independent neutral molecules, **5**, and each consists of one deprotonated ligand L$^-$, one Zn^{II} ion, one Yb^{III} ion, and four chelating acetic groups, two bridging the Zn^{II} and Yb^{III} centers together and the other two coordinating to the Yb^{III} center in a chelating manner (Figure 5). The Zn^{II} and Yb^{III} atoms in **5**, similar to those in **2**, are also pentacoordinated by N2O3 and O8 donor sets, respectively. The ligand HL is ionized to the anionic form L$^-$ because of deprotonation of the phenolic hydroxyl hydrogen atom and is coordinated in a tridentate N2O-bis(chelate) and a bidentate O2-chelate fashion, thus forming three five/six-membered chelate rings. The Zn···Yb separations are close to 3.640 Å. In the crystal, the elements of the structure are connected by intermolecular hydrogen-bonding C−H···O interactions in which pyridine rings and methyl groups act as donors and coordinated acetates as acceptors, finally forming a 3D supramolecular network (Figure S6 and Table S1 in the SI).

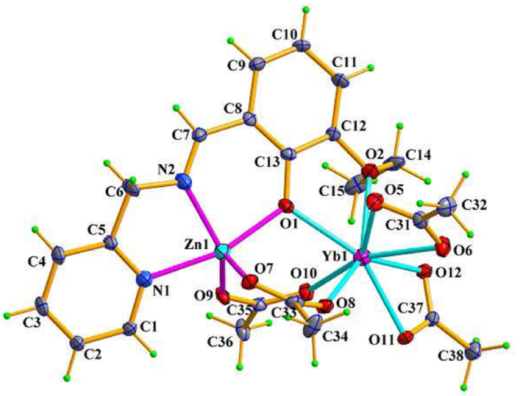

Figure 5. Perspective view of **5** with atomic labels and their displacement ellipsoids at 20% probability.

Structure Transformation and Anion Effect. In this contribution, the Schiff base ligand HL with a donor set of N2O2 was first applied in the field of zinc−lanthanide heterometallic systems. The initial reaction of $Zn(OAc)_2$ with HL afforded trinuclear zinc compound **1** ($[Zn_3L_2]$ core) with two zinc ions of terminal sides coordinated to a donor set of N_2O_2, while the central zinc coordinated to an O6 donor set from two separate ligands and two μ_2-acetates. Provided that nitrogen atoms prefer to coordinate to transitional metals and oxygen atoms are prone to coordinate with lanthanide, when further reacted with $Yb(ClO_4)_3$, the central zinc ions could be easily replaced by lanthanide with additional coordination of one acetic anion to generate compound $[YbZn_2L_2(OAc)_4]\cdot ClO_4$ (**2**; $[Zn_2YbL_2]$ core). On the other hand, the reaction of **1** with $Yb(NO_3)_3$, $YbCl_3$, or $Yb(OAc)_3$ caused destruction of the $[Zn_3L_2]$ core and the subsequent formation of dinuclear compounds **3** ([$YbZnL_2$] core)/**5** ([YbZnL] core) or multinuclear compound **4** ([Yb_4L_4]·Zn) (Scheme 2), respectively.

A careful inspection of the experimental conditions reveals that the anion provided by the lanthanide salt has a significant contribution to the final structure of zinc−ytterbium heterometallic compounds **2**−**5**, which might mainly depend on the variable coordination abilities of ClO_4^-, NO_3^-, Cl^-, and OAc^- to lanthanide ions. The resulting homotrinuclear Zn3 complex **1** with the [Zn_3L_2] core features the central Zn2 atom with an O6 donor environment and two remaining terminal zinc atoms (Zn1 and Zn3) with a N2O2 donor set from two ligands L^- and two μ_2-bridging acetates. Because of the preference of lanthanide for oxygen over nitrogen atoms, **1** as the starting material reacted with YbX_3 (X = ClO_4, NO_3, Cl, OAc) easily leads to the Yb^{III} atom replacing the Zn^{II} atom in an O6 coordination environment to generate heteronuclear Zn^{II}−Yb^{III} complexes. Considering the different coordination abilities of the counterions such as ClO_4^-, NO_3^-, Cl^-, and OAc^- to metal ions, namely, in most cases, the perchloride anion tends not to coordinate with the metal ion, while the nitrate anion inclines to strongly chelate to metal ions, acting as a terminal ligand. As for the chloride ion and acetic group, they often flexibly coordinate with metal ions in terminal or bridging modes. It is not difficult to understand, therefore, that the anion effect plays an important role in the assembly of complexes **2**−**5** with different models under the same reaction conditions, although formation of the final complexes is the synergistic effect from various factors.

Luminescent Properties. As previously stated, zinc−ligand chromophores could be designed as sensitizers for Yb^{III}-based NIR luminescence. Considering the influence of the structural changes on the luminescence performance of complexes, the luminescent properties of five complexes, **1**−**5**, and ligand HL were investigated at room temperature. UV−vis absorption spectra of **1**−**5** in MeCN show some red shifting with 3408, 2705, 1258, 1962, and 2559 cm^{-1} compared to the absorption bands at 338 nm (29586 cm^{-1}) of HL, respectively (Figure 6).

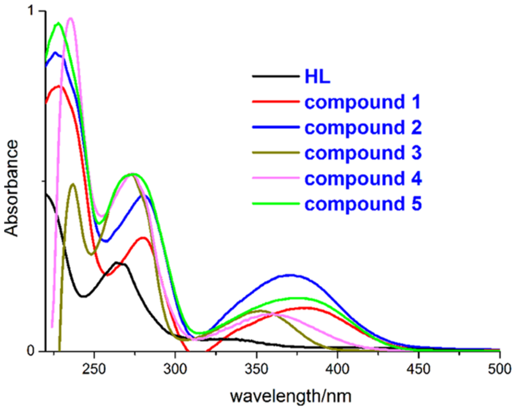

Figure 6. UV−vis absorption spectra of free ligand HL and complexes **1**−**5** in MeCN (concentrations: 1 × 10^{-5} M).

From Figure 7, four complexes, **2**−**5**, containing Yb^{III} atoms show typical NIR emission bands of Yb^{3+} assigned to the $^2F_{5/2} \rightarrow {}^2F_{7/2}$ transitions at a wavelength of 980 nm upon excitation of the zinc−ligand-centered absorption band with emission lifetimes of 8.86, 7.23, 3.89, and 6.98 μs. So, the intrinsic quantum yields of Yb^{3+} emission in **2**−**5** are calculated as 0.44, 0.36, 0.19, and 0.35%, respectively (Table 1). However, different maximum bands in excitation spectra with λ_{ex} = 370 nm for **2**, **3**, and **5** and λ_{ex} = 330 nm for **4** hint at different predominant energy-transfer pathways for the four complexes, which is further supported by their crystal structures and UV−vis absorption spectra, as well as the computational simulation of UV absorption spectra for **2**, according to which the absorbance band at around 370 nm could be assigned to the electron transition from HOMO−5 to LUMO, presenting ligand-to-ytterbium charge-transfer (LMCT) and zinc-to-ytterbium charge-transfer (MMCT) excited states (Figure S7 in the SI). Analysis of single-crystal structures shows that per the Yb^{III} ion in **2** was accompanied by two adjacent Zn^{II} ions, while that for **3** was only one Zn^{II} ion. In **4**, the big separation of 8.576 Å between Zn^{II} and Yb^{III} ions blocks the Zn^{II} center, transferring energy to Yb^{III} center. Therefore, in **2**, **3**, and **5**, energy transfer from the zinc−ligand centers to Ln^{3+} ions accounts for most of the energy required for the ytterbium-based NIR luminescence intensity, while the energy of exciting ytterbium-centered luminescence in **4** can only originate from ligand L^-, meaning that zinc−ligand centers as chromophores play a significant role in sensitizing ytterbium-based NIR luminescence. The importance of Zn^{II} ions could also be confirmed, meanwhile, by another fact that compound **2** is almost 50% superior to compound **3** in NIR luminescence

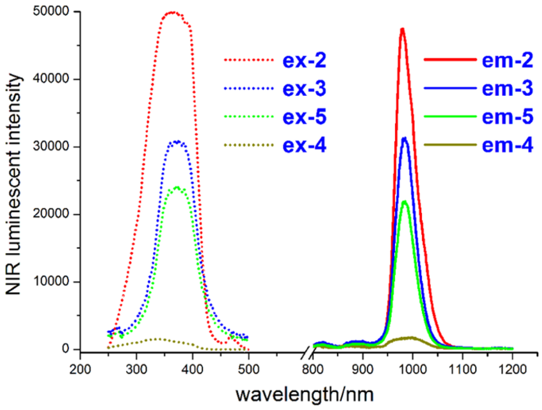

Figure 7. NIR luminescence of complexes **2**−**5** in the solid state.

Table 1. Photophysical Properties of the HL and Complexes 1−5 at 1 × 10^{-5} M in a MeCN Solution (for UV Absorption) or Solid State (for NIR Emission) at Room Temperature

	absorption	excitation	NIR emission
compound/ HL	λ_{max}, nm (log ε, L·mol^{-1}·cm^{-1})	λ_{ex}, nm	λ_{em}, nm (τ, μs; Φ_{Ln}, %)[a]
HL	221 (4.66), 265 (4.41), 338 (3.47)		
1	228 (4.88), 280 (4.51), 382 (4.12)		
2	228 (4.94), 280 (4.66), 370 (4.36)	370	980 (8.86, 0.44)
3	236 (4.69), 271 (4.72), 353 (4.09)	372	980 (7.23, 0.36)
4	235 (4.99), 273 (4.71), 362 (4.02)	369	980 (3.89, 0.19)
5	227 (4.98), 273 (4.72), 376 (4.21)	330	980 (6.98, 0.35)

[a] Intrinsic quantum yields were obtained using equation $\Phi_{Ln} = \tau/\tau_0$ (τ_0 = 2000 μs, the natural lifetime of Yb^{3+}).[1c,8a]

intensity in the same environment because each Yb^{III} in **2** was accompanied by two Zn^{II} ions while each Yb^{III} in **3** was accompanied by one Zn^{II}. Moreover, two μ_3-bridging water molecules coordinated to four Yb^{III} ions, to a certain extent, quench the fluorescence of **4**.[13] The unparalleled ratio of the NIR luminescent intensity (1.5) and ratio of the intrinsic quantum yield (1.2) between complexes **2** and **3** may originate from the intersystem crossing efficiency (population of the ligand's triplet state) and (or) from the energy-transfer efficiency (energy gap between the ligand's triplet excited state and the accepting Yb^{III} level, $^2F_{5/2}$). The efficiencies of these two photophysical processes may be different in these two complexes. From the above analyses and discussion, nevertheless, we can still conclude that the NIR luminescence properties of complexes **2**−**5** are closely related to their structure models.

On the other hand, the visible luminescence spectra of **1**−**5** and HL showed zinc/ligand-centered emission at about 464 nm upon excitation of the ligand-centered absorption bands (Figure 8). The decreasing order of their luminescent intensity at 464 nm is **1** > **4** > **5** > **3** > **2** > HL, indicating the efficiency of energy transfer from the zinc/ligand center to the Yb^{3+} energy level as **2** > **3** > **5** > **4**, in agreement with the NIR luminescent intensity of **2**−**5**.

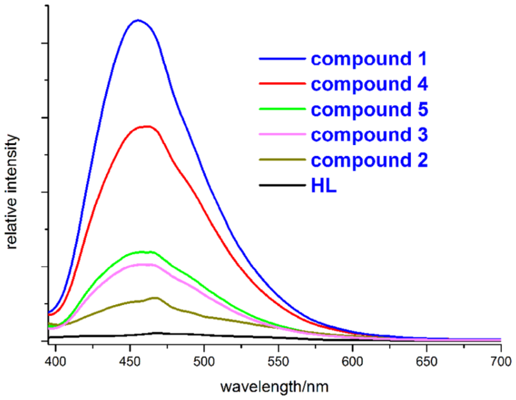

Figure 8. Visible emission spectra of **1**−**4** and ligand HL in the solid state (λ_{ex} = 330 nm).

In order to investigate substitution of the central Zn^{II} ion with the Yb^{III} ion in solution, the visible and NIR luminescent spectra of **1** in CH_3CN at room temperature upon stepwise titration of $Yb(ClO_4)_3$ were studied. The results revealed that, with the concentration of Yb^{3+} gradually increasing, the ligand-centered emission at 473 nm gradually blue-shifted to 460 nm with intensity quenching, while the emission at 980 nm was enhanced little by little, darkening the blue emission of the solution under UV radiation (Figure 9). Evidently, spectral change could be attributed to substitution of the central Zn^{II} by Yb^{III} and energy transfer from the zinc/ligand center to the Yb^{III} atom. As a control experiment, a similar reaction, in which $Tb(ClO_4)_3$ replacing $Yb(ClO_4)_3$ reacted with complex **1**, could also generate zinc−terbium heterometallic complex **6** similarly to **2** (Figure S8 and Table S2 in the SI), which presents a terbium-typical emission in CH_3CN (0.1 mM) with an emission lifetime at 547 nm of 0.5 ms (Φ_{em} = 18.9%).[14] Titration of Zn3 complex **1** in CH_3CN with $Tb(ClO_4)_3$ could lead to quenching of its ligand-centered emission and enhancement of the typical Tb^{3+} luminescence attributable to $^5D_4 \rightarrow {}^7F_n$ transitions (n = 6, 5, 4, and 3), with the color of solution changing from blue to green under irradiation of UV light (Figure 10). Moreover, quenching of ligand-centered

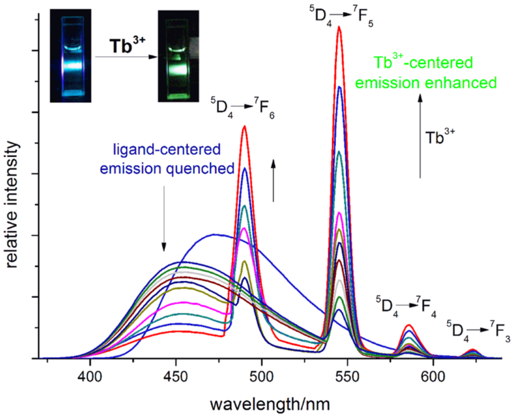

Figure 10. Zinc/ligand-centered luminescence quenching and the terbium-typical luminescence enhancement of **1** (0.1 mM) upon the stepwise addition of $Tb(ClO_4)_3$ (0, 0.1, 0.2, 0.3, 0.4, 0.5, 0.6, 0.7, 0.8, 0.9, and 1.0 equiv) in CH_3CN (λ_{ex} = 370 nm).

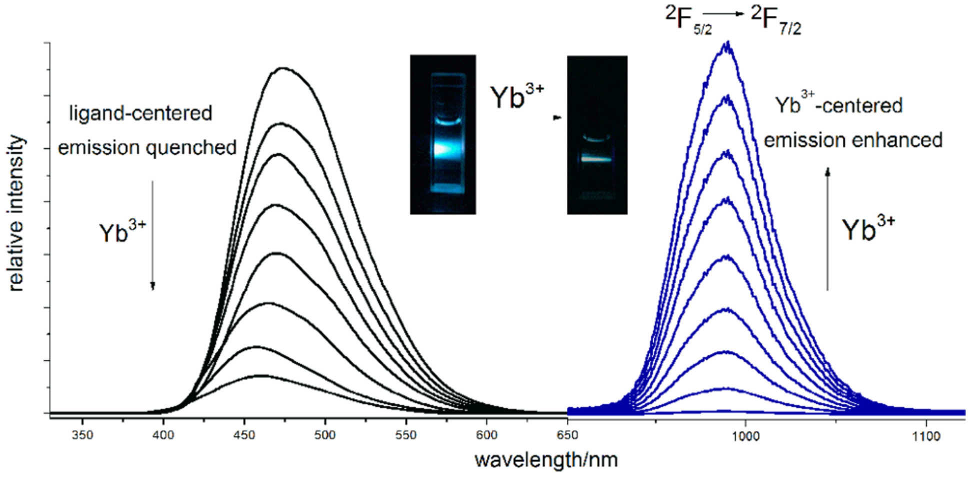

Figure 9. Zinc/ligand-centered luminescence quenching at λ_{em} = 454 nm and ytterbium-based NIR luminescence enhancement at λ_{em} = 980 nm of **1** (0.1 mM) upon the stepwise addition of $Yb(ClO_4)_3$ (0, 0.1, 0.2, 0.3, 0.4, 0.5, 0.6, 0.7, and 0.8 equiv) in CH_3CN (λ_{ex} = 370 nm).

emission could not be observed when more than 1 equiv of $Ln(ClO_4)_3$ (Ln = Yb, Tb) is added, which indicates a 1:1 binding ratio between **1** and Tb^{3+}/Yb^{3+}. Therefore, the spectral change of **1** upon titration of Tb^{3+} or Yb^{3+} in a CH_3CN solution indicated that **1** could be potential dual-wavelength fluorescent probes for Tb^{3+} or Yb^{3+} ions.

3. EXPERIMENTAL SECTION

General Procedures. All chemicals were of analytical reagent grade and were used as received without any further purification. Elemental analysis for carbon, hydrogen, and nitrogen were performed on a PerkinElmer 2400 analyzer. IR spectra were recorded with a PerkinElmer Fourier transform infrared spectrophotometer with samples prepared as KBr disks in the 4000−400 cm^{-1} range.

X-ray Crystallography. Data collections were performed at 298 K on a Bruker Smart Apex II diffractometer with graphite-monochromated Mo Kα radiation (λ = 0.71073 Å) for six compounds, **1**−**6**. Absorption corrections were applied by using the multiscan program *SADABS*.[15] Structural solutions and full-matrix least-squares refinements based on F^2 were performed with the *SHELXS-97*[16] and *SHELXL-97*[17] program packages, respectively. All of the non-hydrogen atoms were refined anisotropically. The hydrogen atoms on organic motifs were placed at calculated positions, and all water hydrogen atoms were located from difference maps and refined with isotropic temperature factors. Details of the crystal parameters, data collections, and refinements for complexes **1**−**6** are summarized in Table S2 in the SI. Selected bond lengths and angles of complexes **1**−**6** are shown in Table S3 in the SI. Hydrogen-bond parameters of complexes **1**−**6** are listed in Table S1 in the SI. CCDC 991995−992000 are for the six new compounds **1**−**6**, respectively. These data can be obtained free of charge from The Cambridge Crystallographic Data Centre via www.ccdc.cam.ac.uk/data_request/cif.

UV−Vis−NIR Spectral Measurement. UV−vis absorption spectra were recorded on a Shimadzu UV1800 UV−vis spectrophotometer. Vis−NIR fluorescent spectra were recorded on an Edinburg FLS 920 spectrometer with an excitation slit of 9.8 nm and an emission slit of 10.8 nm.

Computational Methodology. The singlet ground electronic state (S_0) and the first excited triplet state (T_1) were performed on time-dependent density functional theory calculations based on the experimental model of complex **2** without structural optimization. The ECP28MWB pseudopotential was employed for the ytterbium atom, while the 6-311+G* basis set was employed for carbon, hydrogen, nitrogen, and oxygen atoms. All of the calculations were performed using the *Gaussian 03* program package (revision B.01).[18]

Synthesis of HL. The Schiff base ligand 2-ethoxy-6-[(pyridin-2-ylmethylimino)methyl]phenol (HL) was synthesized by a condensation reaction between pyridin-2-ylmethanamine (1.03 mL, 10 mmol) and 3-ethoxy-2-hydroxybenzaldehyde (1.64 g, 10 mmol) in methanol (50 mL) through refluxing at 60 °C for 1 h. Excess methanol was removed by rotary evaporation to obtain a yellow oil, which was purified by silica gel column chromatography using CH_2Cl_2/methanol (10:1, v/v) as the eluent to afford the ligand HL. Yield: 1.93 g (75.4%). Elem anal. Calcd for $C_{15}H_{16}N_2O_2$: C, 70.29; H, 6.29; N, 10.93. Found: C, 70.18; H, 6.35; N, 10.97. ^1H NMR (DMSO-d_6, 400 MHz, $Si(CH_3)_4$): δ 8.62 (N═CH− and pyridine-H, m, 2H), 8.07 (pyridine-H, s, 1H), 7.56 (m, 2H), 6.84 (d, 2H), 6.36 (m,1H), 5.04 (s,1H), 4.35 (m,1H), 3.95 ($-CH_2-$, t, 2H), 1.34 ($-CH_3$, t, 3H). ^{13}C NMR (DMSO-d_6, 100 MHz): δ 169.98, 162.19, 156.28, 151.39, 148.16, 139.83, 126.84, 123.60, 118.25, 115.04, 112.05, 63.25, 56.49, 18.78, 15.23.

Synthesis of Compounds 1−6. *$\{[(Zn(OAc)(H_2O)L]_2Zn\}(ClO_4)_2\cdot 4H_2O$ (**1**).* After refluxing at 60 °C for 1 h, to a mixed solution of 3-ethoxy-2-hydroxybenzaldehyde (0.2 mmol, 33.2 mg) and 2-pyridin-2-ylmethanamine (0.2 mmol 21 uL) in MeOH (20 mL) was added $Zn(OAc)_2$ (0.2 mmol, 44 mg), $NaClO_4$ (0.2 mmol, 28 mg), and Et_3N (0.2 mmol, 76 μL) with stirring. The resulting clear yellow solution was stirred for 1 h more and then filtered. After 1 week, pale-yellow needle-shaped crystals of complex **1** were obtained after slow evaporation of the resulting clear solution. Yield [based on $Zn(OAc)_2$]: 43.9 mg (30%). IR (KBr, cm^{-1}): 3527 (m), 2960 (w), 2067 (w), 1654 (s), 1571 (s), 1409 (s), 1328 (m), 1149 (m), 1118 (m), 777 (m), 621 (w), 516 (m). Elem anal. Calcd for $C_{34}H_{48}Cl_2N_4O_{20}Zn_3$: C, 37.13; H, 4.40; N, 5.09. Found: C, 37.44; H, 4.57; N, 5.01.

*$[YbZn_2L_2(OAc)_4]\cdot ClO_4$ (**2**).* After refluxing at 60 °C for 1 h, to a mixed solution of 3-ethoxy-2-hydroxybenzaldehyde (0.2 mmol, 33.2 mg) and 2-pyridin-2-ylmethanamine (0.2 mmol 21uL) in MeOH (20 mL) was added $Zn(OAc)_2$ (0.2 mmol, 44 mg) and Et_3N (0.2 mmol, 76 μL) with stirring. The resulting clear yellow solution was stirred for 1 h more, and then $Yb(ClO_4)_3\cdot 6H_2O$ (0.1 mmol, 59 mg) was added and the solution was stirred for 2 h more. After 1 week, pale-yellow needle-shaped crystals of **2** were obtained after slow evaporation of the resulting clear solution. Yield [based on $Yb(ClO_4)_3\cdot 6H_2O$]: 38.7 mg (26%). IR (KBr, cm^{-1}): 3446 (m), 2666 (w), 2370 (w), 1645 (s), 1566 (s), 1423 (s), 1328 (m), 1215 (m), 1118 (m), 779 (m), 623 (w), 516 (w). Elem anal. Calcd for $C_{38}H_{42}ClN_4O_{16}YbZn_2$: C, 39.69; H, 3.68; N, 4.87. Found: C, 39.59; H, 3.72; N, 4.88.

*$YbZnL_2(NO_3)_3$ (**3**).* The procedure was the same as that for **2** using $Yb(NO_3)_3\cdot 5H_2O$ (45.2 mg, 0.1 mmol). Pale-yellow single crystals of **3** formed in 2 weeks. Yield [based on $Yb(NO_3)_3\cdot 5H_2O$]: 39.4 mg (42%). IR (KBr, cm^{-1}): 3431 (m), 2956 (w), 2384 (w), 1645 (s), 1570 (s), 1508 (m), 1419 (s), 1327 (m), 1278 (m), 1219 (m), 1039 (w), 779 (m), 746 (w), 516 (m). Elem anal. Calcd for $C_{30}H_{30}N_7O_{13}YbZn$: C, 38.54; H, 3.23; N, 10.49. Found: C, 38.57; H, 3.27; N, 10.43.

*$[(YbL)_2(H_2O)Cl(OAc)]_2[ZnCl_4]_2$ (**4**).* The procedure was the same as that for **2** using $YbCl_3\cdot 6H_2O$ (38.7 mg, 0.1 mmol). Pale-yellow single crystals of **4** formed in 2 weeks. Yield (based on $YbCl_3\cdot 6H_2O$): 24.4 mg (43%). IR (KBr, cm^{-1}): 3412 (m), 2956 (w), 2378 (w), 1645 (s), 1571 (m), 1419 (s), 1328 (m), 1149 (w), 1012 (m), 931 (w), 885 (w), 779 (m), 653 (w), 516 (m). Elem anal. Calcd for $C_{32}H_{37}Cl_5N_4O_8Yb_2Zn$: C, 32.18; H, 3.12; N, 4.69. Found: C, 32.25; H, 3.07; N, 4.71.

*$YbZnL(OAc)_4$ (**5**).* The procedure was the same as that for **2** using $Yb(OAc)_3\cdot 4H_2O$ (42.2 mg, 0.1 mmol). Pale-yellow single crystals of **5** formed in 2 weeks. Yield [based on $Yb(OAc)_3\cdot 4H_2O$]: 24.0 mg (33%). IR (KBr, cm^{-1}): 3445 (m), 2956 (m), 2372 (w), 2069 (s), 1641 (s), 1570 (s), 1419 (s), 1328 (m), 1151 (s), 1012 (w), 779 (m), 650 (m), 750 (w), 516 (ms). Elem anal. Calcd for $C_{23}H_{24.5}N_2O_{10}YbZn$: C, 37.98; H, 3.39; N, 3.85. Found: C, 37.86; H, 3.34; N, 3.90.

*$\{[(Zn(OAc)_2L]_2Tb\}ClO_4$ (**6**).* The procedure was the same as that for **2** using $Tb(ClO_4)\cdot 6H_2O$ (56.5 mg, 0.1 mmol). Pale-yellow single crystals of **6** formed in 2 weeks. Yield [based on $Tb(ClO_4)_3\cdot 6H_2O$]: 53.4 mg (46%). IR (KBr, cm^{-1}): 3446 (m), 2666 (w), 2370 (w), 1645 (s), 1566 (s), 1423 (s), 1328 (m), 1215 (m), 1118 (m), 779 (m), 623 (w), 516 (w). Elem anal. Calcd for $C_{38}H_{42}ClN_4O_{16}TbZn_2$: C, 40.18; H, 3.73; N, 4.93. Found: C, 40.12; H, 3.76; N, 4.93.

Caution! *Metal perchlorate salts should be handled in small quantities and with extreme care because they might cause explosion.*

4. CONCLUSION

In summary, by the successful assembly of complexes **1**−**5**, we have systematically demonstrated the anion effect on the assembly of heteronuclear $Zn^{II}-Yb^{III}$ complexes in a Schiff base system with pyridine and *o*-ethylvanillin substituents for the first time, in which the Zn^{II}-sensitized NIR luminescent performances in four complexes, **2**−**5**, are closely related to their structural models. Meanwhile, the spectral change of **1** upon titration of Tb^{3+} or Yb^{3+} in a CH_3CN solution shows that **1** could be potential dual-wavelength fluorescent probes for Tb^{3+} or Yb^{3+} ions.

■ ASSOCIATED CONTENT

Ⓢ Supporting Information

Details for crystal data in Tables S1−S3, additional Figures S1−S11, and CIF file containing X-ray crystallographic data for 1−

6. This material is available free of charge via the Internet at http://pubs.acs.org.

■ AUTHOR INFORMATION

Corresponding Author

*E-mail: caiyp@scnu.edu.cn. Tel: +86-020-39310383. Fax: +86-020-39310.

Notes

The authors declare no competing financial interest.

■ ACKNOWLEDGMENTS

This work has been supported by the National Natural Science Foundation of China (Grants 91122008 and 21071056), Research Fund for the Doctoral Program of Higher Education of China (Grant 20124407110007), Guangdong Province of Higher School Science and Technology Innovation Key Project (Project cxzd1113), and Foundation for High-level Talents in Higher Education of Guangdong, China (Grant C10301).

■ REFERENCES

(1) (a) Xu, L.-J.; Xu, G.-T.; Chen, Z.-N. *Coord. Chem. Rev.* **2014**, *273–274*, 47–62. (b) Bünzli, J.-C. G.; Piguet, C. *Chem. Soc. Rev.* **2005**, *34*, 1048–1077. (c) Bünzli, J.-C. G. *Chem. Rev.* **2010**, *110*, 2729–2755. (d) Bünzli, J.-C. G. *Acc. Chem. Res.* **2006**, *39*, 53–61. (e) Eliseeva, S. V.; Bünzli, J.-C. G. *Chem. Soc. Rev.* **2010**, *39*, 189–227. (f) Binnemans, K. *Chem. Rev.* **2009**, *109*, 4283–4374.

(2) (a) Wong, W.-K.; Zhu, X.; Wong, W.-Y. *Coord. Chem. Rev.* **2007**, *251*, 2386–2399. (b) DÁléo, A.; Pointillart, F.; Ouahab, L.; Andraud, C.; Maury, O. *Coord. Chem. Rev.* **2012**, *256*, 1604–1620.

(3) (a) Aboshyan-Sorgho, L.; Nozary, H.; Aebischer, A.; Bunzli, J.-C. G.; Morgantini, P.-Y.; Kittilstved, K. R.; Hauser, A.; Eliseeva, S. V.; Petoud, S.; Piguet, C. *J. Am. Chem. Soc.* **2012**, *134*, 12675–12684. (b) Imbert, D.; Cantuel, M.; Bünzli, J.-C. G.; Bernardinelli, G.; Piguet, C. *J. Am. Chem. Soc.* **2003**, *125*, 15698–15699. (c) Sorgho, L. A.; Besnard, C.; Pattison, P.; Kittilstved, K. R.; Aebischer, A.; Bunzli, J.-C. G.; Hauser, A.; Piguet, C. *Angew. Chem., Int. Ed.* **2011**, *50*, 4108–4112.

(4) (a) Tropiano, M.; Kilah, N. L.; Morten, M.; Rahman, H.; Davis, J. J.; Beer, P. D.; Faulkner, S. *J. Am. Chem. Soc.* **2011**, *133*, 11847–11849. (b) Yuan, Y.-F.; Cardinaels, T.; Lunstroot, K.; Hecke, K. V.; Meervelt, L. V.; Gorller-Walrand, C.; Binnemans, K.; Nockemann, P. *Inorg. Chem.* **2007**, *46*, 5302–5309. (c) Dehaen, G.; Verwilst, P.; Eliseeva, S. V.; Laurent, S.; Elst, L. V.; Muller, R.; Borggraeve, W. M. D.; Binnemans, K.; Parac-Vogt, T. N. *Inorg. Chem.* **2011**, *50*, 10005–10014. (d) Nonat, A. M.; Allain, C.; Faulkner, S.; Gunnlaugsson, T. *Inorg. Chem.* **2010**, *49*, 8449–8456. (e) Charbonnière, L. J.; Faulkner, S.; Platas-Iglesias, C.; Regueiro-Figueroa, M.; Nonat, A.; Rodríguez-Blas, T.; de Blas, A.; Perryd, W. S.; Tropiano, M. *Dalton Trans.* **2013**, *42*, 3667–3681. (f) Tropiano, M.; Record, C. J.; Morris, E.; Rai, H. S.; Allain, C.; Faulkner, S. *Organometallics* **2012**, *31*, 5673–5676. (g) Wei, Q.-H.; Lei, Y.-F.; Xu, W.-R.; Xie, J.-M.; Chen, G.-N. *Dalton Trans.* **2012**, *41*, 11219–11225. (h) Piazza, E. D.; Norel, L.; Costuas, K.; Bourdolle, A.; Maury, O.; Rigaut, S. *J. Am. Chem. Soc.* **2011**, *133*, 6174–6176.

(5) (a) Chen, Z.-Q.; Ding, F.; Bian, Z.-Q.; Huang, C.-H. *Org. Electron.* **2010**, *11*, 369–376. (b) Lian, P.; Wei, H.; Zheng, C.; Nie, Y.; Bian, J.; Bian, Z.; Huang, C. *Dalton Trans.* **2011**, *40*, 5476–5482. (c) Jiang, W.; Lou, B.; Wang, J.; Lv, H.; Bian, Z.; Huang, C. *Dalton Trans.* **2011**, *40*, 11410–11418. (d) Ali, N. M.; MacLeod, V. L.; Jennison, P.; Sazanovich, I. V.; Hunter, C. A.; Weinstein, J. A.; Ward, M. D. *Dalton Trans.* **2012**, *41*, 2408–2419. (e) Tart, N. M.; Sykes, D.; Sazanovich, I.; Tidmarsh, I. S.; Ward, M. D. *Photochem. Photobiol. Sci.* **2010**, *9*, 886–889. (f) Sykes, D.; Tidmarsh, I. S.; Barbieri, A.; Sazanovich, I. V.; Weinstein, J. A.; Ward, M. D. *Inorg. Chem.* **2011**, *50*, 11323–11339. (g) Sykes, D.; Ward, M. D. *Chem. Commun.* **2011**, *47*, 2279–2281. (h) Edkins, R. M.; Sykes, D.; Beeby, A.; Ward, M. D. *Chem. Commun.* **2012**, *48*, 9977–9979. (i) Jones, J. E.; Jenkins, R. L.; Hicks, R. S.; Hallett, A. J.; Pope, S. J. A. *Dalton Trans.* **2012**, *41*, 10372–10381.

(6) (a) Guenet, A.; Eckes, F.; Bulach, V.; Strassert, C. A.; De Cola, L.; Hosseini, M. W. *ChemPhysChem* **2012**, *13*, 3163–3171. (b) Li, J.; Wang, J.-Y.; Chen, Z.-N. *J. Mater. Chem. C* **2013**, *1*, 3661–3668.

(7) (a) Abtab, S. M. T.; Audhya, A.; Kundu, N.; Samanta, S. K.; Sardar, P. S.; Butcher, R. J.; Ghosh, S.; Chaudhury, M. *Dalton Trans.* **2013**, *42*, 1848–1861. (b) Pasatoiu, T. D.; Tiseanu, C.; Madalan, A. M.; Jurca, B.; Duhayon, C.; Sutter, J. P.; Andruh, M. *Inorg. Chem.* **2011**, *50*, 5879. (c) Zhao, S.; Liu, X.; Lu, X.; Wong, W.-k. *Spectrosc. Lett.* **2013**, *46*, 109. (d) Xu, H.-B.; Zhong, Y.-T.; Zhang, W.-X.; Chen, Z.-N.; Chen, X.-M. *Dalton Trans.* **2010**, *39*, 5676–5682. (e) Xu, H.-B.; Wen, H.-M.; Chen, Z.-H.; Li, J.; Shi, L.-X.; Chen, Z.-N. *Dalton Trans.* **2010**, *39*, 1948–1953.

(8) (a) Yang, X.-P.; Schipper, D.; Jones, R. A.; Lytwak, L. A.; Holliday, B. J.; Huang, S. *J. Am. Chem. Soc.* **2013**, *135*, 8468–8471. (b) Fang, H.-C.; Zhu, J.-Q.; Zhou, L.-J.; Jia, H.-Y.; Li, S.-S.; Gong, X.; Li, S.-B.; Cai, Y.-P.; Thallapally, P. K.; Liu, J.; Exarhos, G. J. *Cryst. Growth Des.* **2010**, *10*, 3277–3284.

(9) (a) Lemonnier, J.-F.; Guénée, L.; Beuchat, C.; Wesolowski, T. A.; Mukherjee, P.; Waldeck, D. H.; Gogick, K. A.; Petoud, S.; Piguet, C. *J. Am. Chem. Soc.* **2011**, *133*, 16219–16234. (b) Lo, W.-K.; Wong, W.-K.; Wong, W.-Y.; Guo, J.-P.; Yeung, K.-T.; Cheng, Y.-K.; Yang, X.-P.; Jones, R. A. *Inorg. Chem.* **2006**, *45*, 9315–9325. (c) Su, K.-Z.; Jiang, F.-L.; Qian, J.-J.; Wu, M.-Y.; Xiong, K.-C.; Gai, Y.-L; Hong, M.-C. *Inorg. Chem.* **2013**, *52*, 3780–3786. (d) Lü, X.-Q.; Bi, W.-Y.; Chai, W.-L.; Song, J.-R.; Meng, J.-X.; Wong, W.-Y.; Wong, W.-K.; Jones, R. A. *New J. Chem.* **2008**, *32*, 127–131. (e) Yang, X.-P.; Jones, R. A.; Wong, W.-K.; Lynch, V.; Oyec, M. M.; Holmes, A. L. *Chem. Commun.* **2006**, 1836–1838.

(10) Zhou, X.-X.; Cai, Y.-P.; Zhu, S.-Z.; Zhan, Q.-G.; Liu, M.-S.; Zhou, Z.-Y.; Chen, L. *Cryst. Growth Des.* **2008**, *8*, 2076–2079.

(11) (a) Yang, X.-P.; Jones, R. A.; Huang, S.-M. *Coord. Chem. Rev.* **2014**, *273–274*, 63–75. (b) Sakamoto, M.; Manseki, K.; Okawa, H. *Coord. Chem. Rev.* **2001**, *219*, 379–414. (c) Camp, C.; Guidal, V.; Biswas, B.; Pecaut, J.; Dubois, L.; Mazzanti, M. *Chem. Sci.* **2012**, *3*, 2433–2438. (d) Magadur, G.; Bouanis, F.; Norman, E.; Guillot, R.; Lauret, J.-S.; Huc, V.; Cojocaru, C.-S.; Mallah, T. *Chem. Commun.* **2012**, *48*, 9071–9073. (e) Zhao, L.; Xue, S.; Tang, J. *Inorg. Chem.* **2012**, *51*, 5994–5996. (f) Yang, X.-P.; Michael, M. O.; Jones, R. A.; Huang, S.-M. *Chem. Commun.* **2013**, *49*, 9579–9581.

(12) Bhattacharyya, P.; Parr, J.; Slawin, A. M. Z. *J. Chem. Soc., Dalton Trans.* **1998**, 3263–3268.

(13) (a) Beeby, A.; Clarkson, I. M.; Dickins, R. S.; Faulkner, S.; Parker, D. *J. Chem. Soc., Perkin Trans.* **1999**, *2*, 493–503. (b) Parker, D. *Coord. Chem. Rev.* **2000**, *205*, 109–130.

(14) The overall quantum yield was determined using quinine sulfate (Φ_{em} = 0.546 in 0.5 M H_2SO_4) as the standard for the Tb^{3+} complex **6**: Yang, X.-P.; Jones, R. A. *J. Am. Chem. Soc.* **2005**, *127*, 7686–7687 Value of the relative emission intensity (complex **6** vs quinine sulfate; 298 K) at 547 nm in CH_3CN: 15.2.

(15) Sheldrick, G. M. *SADABS*, version 2.05; University of Göttingen: Göttingen, Germany, 1996.

(16) Sheldrick, G. M. *SHELXS-97, Program for X-ray Crystal Structure Determination*; University of Göttingen: Göttingen, Germany, 1997.

(17) Sheldrick, G. M. *SHELXS-97, Program for X-ray Crystal Structure Refinement*; University of Göttingen: Göttingen, Germany, 1997.

(18) Frisch, M. J.; Trucks, G. W.; Schlegel, H. B.; Scuseria, G. E.; Robb, M. A.; Cheeseman, J. R.; Montgomery, J. A., Jr.; Vreven, J. T.; Kudin, K. N.; Burant, J. C.; Millam, J. M.; Iyengar, S. S.; Tomasi, J.; Barone, V.; Mennucci, B.; Cossi, M.; Scalmani, G.; Rega, N.; Petersson, G. A.; Nakatsuji, H.; Hada, M.; Ehara, M.; Toyota, K.; Fukuda, R.; Hasegawa, J.; Ishida, M.; Nakajima, T.; Honda, Y.; Kitao, O.; Nakai, H.; Klene, M.; Li, X.; Knox, J. E.; Hratchian, H. P.; Cross, J. B.; Adamo, C.; Jaramillo, J.; Gomperts, R.; Stratmann, R. E.; Yazyev, O.; Austin, A. J.; Cammi, R.; Pomelli, C.; Ochterski, J. W.; Ayala, P. Y.; Orokuma, K.; Voth, G. A.; Salvador, P.; Dannenberg, J. J.; Zakrzewski, V. G.; Dapprich, S.; Daniels, A. D.; Strain, M. C.; Farkas, O.; Malick, D. K.; Rabuck, A. D.; Raghavachari, K.; Foresman, J. B.; Ortiz, J. V.;

Cui, Q.; Aboul, A. G.; Clifford, S.; Cioslowski, J.; Stefanov, B. B.; Liu, G.; Liashenko, A.;Piskorz, P.; Komaromi, I.; Martin, R. L.; Fox, D. J.; Keith, T.; AlLaham, M. A.; Peng, C. Y.; Nanayakkara, A.; Challacombe, M.; Gill, P. M. W.; Johnson, B.; Chen, W.; Wong, M. W.; Gonzalez, C.; Pople, J. A. *Gaussian 03*, revision B.03; Gaussian, Inc.: Pittsburgh, PA, 2003.